

## Carbon nitride assisted chemoselective C–H bond photo-oxidation of alkylphenoxyethoxylates in water medium†

M. Ilkaeva,<sup>a</sup> I. Krivtsov,<sup>\*a,b</sup> E. Bartashevich,<sup>c</sup> S.A. Khainakov,<sup>d</sup> J.R. García,<sup>a</sup> E. Díaz,<sup>e</sup> S. Ordóñez<sup>e</sup>

Received 00th January 20xx,  
Accepted 00th January 20xx

DOI: 10.1039/x0xx00000x

www.rsc.org/

**The unprecedented ability of g-C<sub>3</sub>N<sub>4</sub> to chemoselectively photo-oxidise the methyl group of 2-(4-methylphenoxy)ethanol instead of the easily oxidised oxyethanol fragment has been demonstrated. When g-C<sub>3</sub>N<sub>4</sub> is treated by H<sub>2</sub>O<sub>2</sub>, its selectivity enhances due to the blocking of surface sites responsible for the adsorption and subsequent oxidation of oxyethanol substituent.**

Selective oxidation of methyl group substituent of aromatic compounds to the corresponding carbonyl and carboxyl functionalities is a process of an immense importance for activation of raw materials in organic synthesis.<sup>1</sup> C–H bond oxidation of alkyl side-chains in aromatic hydrocarbons is well-developed, and many catalytic approaches are successfully applied for this purpose.<sup>2</sup> The presence of competitive easily oxidised substituents in a benzyl ring such as electron-donating –C–OH, –C=O, –O–C, or –NH<sub>2</sub> groups complicates achieving activation of a more inert C–H bond. Thus, a variety of methods utilizing homogeneous oxidation,<sup>3</sup> photoactive complexes,<sup>4</sup> metal oxide-supported noble metal nanoparticles,<sup>5</sup> enzymes<sup>6</sup> and electrochemical oxidation in ionic liquids<sup>7</sup> is developed to overcome this obstacle. Many of the existing oxidation protocols are complicated and expensive, they often demand the presence of toxic oxidants and/or organic solvents, and external heat must be supplied for the reaction to take place. Hence, they are energy consuming and not environmentally benign.

Use of molecular oxygen as a green oxidant and UV or visible-light irradiation as an energy source for partial oxidation of

organic molecules along with application of inexpensive, non-toxic, easily recoverable and zero-waste semiconductor photocatalysts such as TiO<sub>2</sub> or g-C<sub>3</sub>N<sub>4</sub> have recently attracted attention.<sup>8</sup> So far the published data on photo-conversion of organic molecules in the presence of semiconductor photocatalysts are limited to the oxidation of the hydroxyl group of aromatic and aliphatic alcohols to the carbonyl group,<sup>9</sup> sulfides to sulfoxides<sup>10</sup>, and by the oxidation of benzene or the alkyl group of hydrocarbon compounds.<sup>11</sup> Although Verma et al. reported that carbon nitride promoted photo-oxidation of C–H groups of substituted toluenes, they stated that g-C<sub>3</sub>N<sub>4</sub> was not active in the absence of vanadium oxide and H<sub>2</sub>O<sub>2</sub>.<sup>11a</sup>

The diversification of benign and energy-saving oxidation process such as photocatalysis is of utmost importance in order to deal with new challenges. Here, we report the unprecedented chemoselective g-C<sub>3</sub>N<sub>4</sub>-promoted photo-oxidation of the methyl group of an amphiphilic molecule 2-(4-methylphenoxy)ethanol (MPET) leading to the formation of 4-(2-hydroxyethoxy)benzaldehyde (HEB) using atmospheric O<sub>2</sub> as an oxidant. MPET has been chosen as a model compound because it allows modelling and assessing its interaction with the photocatalyst surface, having the functional groups of different polarity. Moreover, HEB, the product of this oxidation reaction, finds its application in pharmaceutical production,<sup>12</sup> but is most commonly used as a building block in polymer synthesis for drug delivery.<sup>13</sup> This chemical is normally produced by synthesis in organic solvents with the use of external heat and halogenated compounds,<sup>14</sup> hence the development of greener and more economic methods of its production is of interest.

Comparison of the performance of the two most widespread photocatalysts in MPET photo-oxidation reveals staggering difference in their reaction pathways (Fig. 1). *p*-Cresol and HEB are found to be the principal partially oxidised MPET products, if commercial titania **Aeroxide P25** is used as a photocatalyst.<sup>15</sup> However, the selectivity for both compounds is below 10% (Fig. 1, Table 1), which is obviously of interest for environmental purposes,<sup>15</sup> but not for chemical synthesis. Graphitic carbon

<sup>a</sup> Departments of Organic and Inorganic Chemistry, Physical and Analytical Chemistry, University of Oviedo-CINN, 33006 Oviedo, Spain.  
E-mail: [UO247495@uniovi.es](mailto:UO247495@uniovi.es), Tel.: +34 985 103 030.

<sup>b</sup> Nanotechnology Education and Research Center, South Ural State University, 454080 Chelyabinsk, Russia.

<sup>c</sup> Department of Theoretical and Applied Chemistry, South Ural State University, 454080 Chelyabinsk, Russia.

<sup>d</sup> SCTs Facilities, University of Oviedo, 33006 Oviedo, Spain.

<sup>e</sup> Department of Chemical and Environmental Engineering, University of Oviedo, 33006 Oviedo, Spain.

† Electronic Supplementary Information (ESI) available. See DOI: 10.1039/x0xx00000x

nitride prepared by direct condensation of melamine at 520 °C (**MCN**), on the other hand, favours producing relatively large quantities of HEB, achieving the selectivity to this product up to 50% (Fig. 1, Table 2). High selectivity observed for the carbon nitride photocatalyst can be explained either by the action of the reactive species generated during the irradiation and different to those produced by TiO<sub>2</sub>, or by the specific interaction of the substrate and photocatalyst surfaces. This question will be addressed later in the communication.

With the purpose of improving the reaction rate and selectivity toward HEB formation we applied several earlier reported treatment procedures. Among them there were thermal exfoliation (**TE**),<sup>16</sup> hydrothermal treatment with NaOH,<sup>17</sup> g-C<sub>3</sub>N<sub>4</sub> protonation with HCl,<sup>18</sup> alkaline metal doping,<sup>19</sup> and H<sub>2</sub>O<sub>2</sub> treatment of the pristine g-C<sub>3</sub>N<sub>4</sub> (**MCN\_O**) similar to that reported by Li et al.,<sup>20</sup> although carried out under milder conditions (for details, see **Supplementary Material**). Some of the g-C<sub>3</sub>N<sub>4</sub> modification methods result in the improved reaction rate, and **TE** sample shows a slight increase of the selectivity, which is due to the partial elimination of uncondensed species,<sup>16b</sup> though a significant enhancement of the HEB production is only observed for **MCN\_O** sample (Fig. S1, Fig. S2), reaching the selectivity value of 87% (Fig. S1).

Obviously, the as-prepared carbon nitride and the one treated by H<sub>2</sub>O<sub>2</sub> are not active enough due to their low specific surface areas (SSA) (Table 3). Thus, g-C<sub>3</sub>N<sub>4</sub> thermal exfoliation at 500 °C (**TE**) and the subsequent H<sub>2</sub>O<sub>2</sub> treatment (**TE\_O**) have been implemented, in order to obtain a more efficient photocatalyst. The apparent reaction rate constant of MPET conversion, showed by **TE** sample, is slightly reduced after the H<sub>2</sub>O<sub>2</sub> treatment (Fig. 2(A), Table 2), while the formation of HEB is noticeably increased (Fig. 2(B)). Although the selectivity toward HEB shows some decrease at high conversion values, it is in the range of 72-83% during the whole time of the reaction (Fig. 2(C,D)).

According to EPR studies reported by Long et al.,<sup>21</sup> the principal reactive species responsible for photo-oxidation of organic molecules by g-C<sub>3</sub>N<sub>4</sub> is a superoxide radical. In this particular case of MPET to HEB photo-oxidation it is confirmed by the application of a set of scavengers for O<sub>2</sub><sup>•-</sup>, OH<sup>•</sup>, photo-generated holes and electrons (Fig. S4). The reaction carried out under N<sub>2</sub> reveals that 14% of MPET is decomposed and no HEB is formed (Fig. S4), which might be a consequence of the direct photo-generated hole oxidation of the substrate and could be the reason for less than 100% selectivity.

The possibility that the active surface species formed in the result of the H<sub>2</sub>O<sub>2</sub> interaction with carbon nitride might be consumed promoting the MPET to HEB oxidation is verified by the utilization of the **TE\_O** photocatalyst in four consecutive cycles (Fig. S5). A slight decrease of the conversion is observed during the photocatalyst reuse, although the selectivity does not suffer any significant changes, demonstrating that there are no H<sub>2</sub>O<sub>2</sub> or other reactive species able to oxidise the substrate consumed during the oxidation, and the nature of the reaction is indeed photocatalytic. Unfortunately, up to now, the attempts to avoid the conversion loss in the reaction cycles have not been successful.

For better understanding of the chemoselectivity of this reaction the analysis of **TE** and **TE\_O**-assisted photo-oxidation products of several other substrate molecules such as 3-(2-methylphenoxy)ethanol, 4-methylbenzyl alcohol, 2-(4-methylphenyl)ethanol, and (4-methylphenoxy)acetic acid has been carried out (Table 1). The position of a methyl group in respect to the competitive oxyethanol fragment has a great effect on the conversion degree and selectivity towards the product of its oxidation. Expectedly, in a view of the results reported by Yurdakal et al. for the case of aromatic alcohols photocatalytic oxidation,<sup>22</sup> the conversion rate, as well as selectivity, is reduced for the case of 3-(2-methylphenoxy)ethanol photo-oxidation to 3-(2-hydroxyethoxy)benzaldehyde. **TE** and **TE\_O** demonstrate nearly equal conversion and selectivity values, which are of 46 % and 39% for **TE**, and 42 and 38 for **TE\_O**, respectively (Fig. S10). The use of **P25** photocatalyst, on the other hand, inevitably leads to formation of *m*-cresol (Fig. S6). Expectedly, g-C<sub>3</sub>N<sub>4</sub> preferably oxidise benzylic OH rather than C-H bond of the methyl group of 4-methylbenzyl alcohol (Fig. S7). The presence in 2-(4-methylphenyl)ethanol of the longer ethanol substituent bearing OH-group on an alkyl carbon atom results in that its photo-conversion produces two products 4-methylbenzaldehyde and 4-(2-hydroxyethyl)benzaldehyde, which are formed by oxidation of the benzylic carbon of the ethanol fragment and the C-H bond of the methyl group, while no alcohol functionality oxidation is observed (Fig. S8). Contrary to that, in the presence of titania **P25 Aeroxide** the oxidation of OH group occurs forming (4-methylphenyl)acetaldehyde (Table 1, Fig. S9). Despite in cases of 2-(4-methylphenyl)ethanol and MPET photo-conversion, C-H bond oxidation takes place, the presence of oxyethanol fragment favours better selectivity for the methyl group oxidation. Nonetheless, the presence of oxyethanol substituent in the substrate molecule does not guarantee the selectivity of the methyl group oxidation. Photocatalytic conversion of (4-methylphenoxy)acetic acid shows low selectivity for methyl group oxidation and demonstrates completely different reaction mechanism producing *p*-cresol and several other unidentified intermediates (Fig. S10). Thus, photo-oxidation of benzylic C-H bond and methyl group occurs also for other class of organic compounds, however the tailoring of selectivity for certain products demands other means of photocatalyst modification.

Since the reactive species responsible for the MPET photo-oxidation to HEB are the same for the **TE** and **TE\_O** samples, it is likely that the interaction of the g-C<sub>3</sub>N<sub>4</sub> surface with MPET governs the selectivity to methyl group oxidation, and the enhancement of the selectivity toward HEB production observed for the carbon nitride treated with H<sub>2</sub>O<sub>2</sub> might be related to the modification of the carbon nitride surface sites. To explore this hypothesis, we have undertaken a detailed study of how the hydrogen peroxide modification influences carbon nitride properties. Contrary to other investigation describing g-C<sub>3</sub>N<sub>4</sub> hydrothermal modification with H<sub>2</sub>O<sub>2</sub>,<sup>20</sup> where the exfoliation and the reduction of crystallinity of carbon nitride were observed, the mild conditions of the treatment applied in this work do not lead to the same result. Surprisingly, the PXRD

pattern of **TE<sub>2</sub>O** shows the intensity increase of the diffraction maxima characteristic of (002) crystallographic plane of *g*-C<sub>3</sub>N<sub>4</sub> phase and its shift from 27.5 to 27.8 degrees indicating the reduction of interplanar distance in *g*-C<sub>3</sub>N<sub>4</sub> (Fig. 3(A)). Higher crystallinity and smaller interplanar distance found for **TE<sub>2</sub>O** is also the cause of the reduced SSA value compared to the thermally exfoliated carbon nitride **TE** (Table 3, Fig. 3(A)). In accordance with it, the XPS data reveal the lower ratio of N-(C)<sub>3</sub> (N<sub>2</sub>) to C=N-C (N<sub>1</sub>) species reflecting the increased condensation degree of the **TE<sub>2</sub>O** sample with respect to **TE** (Table 3, Fig. S11). Expectedly, the changes of the bulk carbon nitride properties after modification by H<sub>2</sub>O<sub>2</sub> affect the electronic structure and photo-generated charge separation of **TE<sub>2</sub>O**. Thus, the absorption edge of **TE<sub>2</sub>O** in respect to that of **TE** is found shifted to the visible-light range (Fig. S12) and the corresponding band-gap (BG) values are estimated to be 2.63 eV with the mid-gap of 2.15 eV for **TE<sub>2</sub>O** and 2.80 eV for **TE** (Table 3, Fig. S12). The treatment by H<sub>2</sub>O<sub>2</sub> suppresses the photoluminescence (PL) of **TE<sub>2</sub>O** (Fig. S13), thus explaining that high photocatalytic activity maintained by H<sub>2</sub>O<sub>2</sub>-treated carbon nitride is due to better charge separation, despite the drastic reduction of SSA.

Apart from the fact that the bulk properties of the material are changed, the treatment also leads to the noticeable modification of the carbon nitride surface. From the XPS surface composition analysis it is seen that the C/N ratio of 0.67 remains unchanged after the treatment, but the oxygen content rises from 3.7 at% for **TE** to 6.3 at% in case of **TE<sub>2</sub>O** (Table 3). Moreover, the O 1s peak in the spectrum of **TE<sub>2</sub>O** shows the shift of the maximum from 532.2 eV, found for **TE**, to 531.8 eV, indicating the existence of different oxygen species to those presented in **TE** (Fig. 3(B)). Recently the melamine-H<sub>2</sub>O<sub>2</sub> (MHP) complex was crystallized and its structure was elucidated by Chernyshov et al.,<sup>23</sup> it was also described by Chehardoli et al. and applied for a controllable homogeneous oxidation.<sup>24</sup> In the present case the formed compound is insoluble and does not release H<sub>2</sub>O<sub>2</sub> while in water or acetonitrile media. <sup>1</sup>H MAS NMR evidences the presence of <sup>1</sup>H (0.55 ppm) most probably belonging to unbridged OH groups<sup>23</sup> at the surface of the **TE** sample, considering that the presence of hydrogenated carbon in *g*-C<sub>3</sub>N<sub>4</sub> is unlike<sup>24</sup> (Fig. 3(C)). This peak is absent on the spectrum of the **TE<sub>2</sub>O** sample, which might be a result of some adsorbed species removal because of SSA reduction or to the surface modification by H<sub>2</sub>O<sub>2</sub>. The maximum at 4.06 ppm apart from NH<sub>2</sub> groups might be attributed to the adsorbed H<sub>2</sub>O, while 8.90 ppm clearly indicates the presence of NH and NH<sub>2</sub> functionalities. The significant shift of both maxima for **TE<sub>2</sub>O** to 4.53 and 9.24 ppm arises from the interaction of the carbon nitride surface species, in particular amino-groups, with hydrogen peroxide (Fig. 3(C)). A characteristic <sup>1</sup>H peak of H<sub>2</sub>O<sub>2</sub> cannot be clearly distinguished because of its possible overlapping with <sup>1</sup>H of the amino-groups. A characteristic <sup>1</sup>H peak of H<sub>2</sub>O<sub>2</sub> cannot be clearly distinguished because of its possible overlapping with <sup>1</sup>H of the amino-groups. The presence of the tri-s-triazine breathing mode at 850-800 cm<sup>-1</sup> indicates that the thermally exfoliated carbon nitride retains the *g*-C<sub>3</sub>N<sub>4</sub> block structure after being treated by hydrogen peroxide (Fig.

S14). The FTIR spectrum of **TE<sub>2</sub>O** presents a number of peak displacements at 1200-1600 and 900-800 cm<sup>-1</sup> corresponding to the changes of interaction between tri-s-triazine units due to the enhanced crystallinity of the sample (Fig. S14). It draws attention to the reduction of the relative intensity of the N-H bond stretching vibration characteristics of primary amines in the range of 3000-3200 cm<sup>-1</sup> for **TE<sub>2</sub>O** with respect to the **TE** FTIR spectrum (Fig. 3(D)), which probably is the consequence of the surface NH<sub>2</sub>-H<sub>2</sub>O<sub>2</sub> complex formation. Thermogravimetric analysis shows the increased mass loss in the low-temperature region for the **TE<sub>2</sub>O** sample, thus confirming the presence of some surface species not presented in the pristine and thermally exfoliated *g*-C<sub>3</sub>N<sub>4</sub> (Fig. S15).

The computational study is indispensable for understanding of the substrate-photocatalyst interactions. It has helped us to confirm the affinity of oxyethanol substituent of MPET to the surface amino-groups and the blockage of these surface sites by one H<sub>2</sub>O<sub>2</sub> molecule. For modelling the features of the carbon nitride interactions with MPET and H<sub>2</sub>O<sub>2</sub> molecules, the simple dimelem fragment representing the terminal surface groups of carbon nitride is chosen. The model structure of the dimelem molecule perfectly shows the presence of the 2D cavity with lateral size ~6 Å between the neighboring nitrogen atoms. Molecular electrostatic potential (MEP) mapped on the iso-surface of the electron density (ED) illustrates pronounced complementarity of nucleophilic and electrophilic fragments in the dimelem cavity and MPET molecule (Fig. S16). The formation of dimelem complexes with polar functional groups of aromatic molecules was earlier suggested by Tan et al.<sup>25</sup> Our calculations demonstrate that MPET forms a stable complex with the dimelem *via* the relatively strong hydrogen bonds between the polar oxyethanol substituent and Nsp<sup>2</sup>-Csp<sup>2</sup>-Nsp<sup>3</sup>-H site (Fig. 4, TableS1). Coordination of MPET in this way would result in its oxidation by the formed radical species or directly *via* photogenerated hole oxidation, thus hindering the formation of the desired product HEB.

One molecule of H<sub>2</sub>O<sub>2</sub> can be attached to the 2D cavity and several molecules of H<sub>2</sub>O<sub>2</sub> are able to form hydrogen bonds with the dimelem nitrogen atoms and amino-groups (Fig. 4). The strength of MPET holding by the direct contacts with the dimelem molecule decreases in this case (Table S1). Thus, the modification of carbon nitride by hydrogen peroxide influences the interactions between dimelem and MPET. Hence, the polar part of MPET becomes protected from the radical attack or direct hole oxidation.

Even the as-prepared *g*-C<sub>3</sub>N<sub>4</sub> has high selectivity to C-H bond oxidation, thus indicating the preferable interaction of oxidant species generated by carbon nitride with the methyl group of MPET. The set of the applied methods has proved the coordination of H<sub>2</sub>O<sub>2</sub> on the carbon nitride surface species. The *g*-C<sub>3</sub>N<sub>4</sub>-H<sub>2</sub>O<sub>2</sub> complex formation creates a steric hindrance for the direct interaction between the polar group of MPET and the amino-groups of carbon nitride. This makes possible suppressing the oxidation of the oxyethanol substituent and enhancing the selectivity of MPET to HEB photo-oxidation even more.

Amphiphilic character of the studied molecule, used in the present study, leads to the favourable oxidation of its methyl

group by g-C<sub>3</sub>N<sub>4</sub>-generated O<sub>2</sub><sup>•-</sup> radicals, thus high values of MPET to HEB selectivity reaching 82% are achieved. The presence of amino-groups on the photocatalyst surface is detrimental to the selectivity to HEB formation, as these species tend to coordinate MPET molecule *via* hydrogen bonding with its polar group and to oxidise it by h<sup>+</sup> or radical species.

The demonstrated extraordinary ability of g-C<sub>3</sub>N<sub>4</sub> to selectively oxidise the alkyl group of alkylphenoletoxyolate and alkyl alcohol molecule in water medium, using O<sub>2</sub> as an oxidant, opens new applications for this unique photocatalyst in the field of organic synthesis. However, in order to get a more profound understanding of the reaction mechanism, it is necessary to test a wider selection of substrates. Moreover, the present study clearly demonstrates that the control of the hydrogen bonding between the functional groups on the photocatalyst surface and the substrate is of paramount importance for the partial photo-oxidation.

## Acknowledgement

This work was financially supported by Spanish MINECO (MAT2013-40950-R, CTQ2014-52956-C3-1-R and MAT2016-78155-C2-1-R) and Gobierno del Principado de Asturias (GRUPIN14-060, GRUPIN14-078 and Severo Ochoa PhD grant BP-14-029 to MI), and FEDER. EB is grateful for the Ministry of Education and Science of the Russian Federation (grant 4.1157.2017/PP).

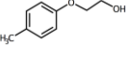
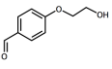
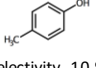
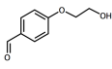
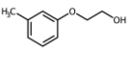
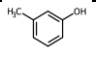
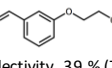
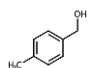
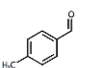
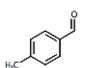
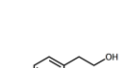
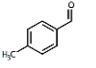
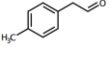
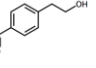
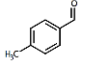
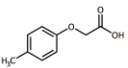
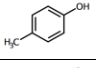
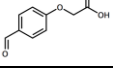
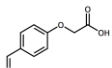
## Notes and references

- 1 *Comprehensive Organic Transformations: A Guide to Functional Group Preparations*, ed. R. C. Larock, Wiley-VCH, New York, 1999.
- 2 (a)L. Kesevan, R. Tiruvalam, M.H. Ab Rahim, M.I. bin Saiman, D.I. Enache, R.L. Jenkins, N. Dimitratos, J.A. López-Sánchez, S.H. Taylor, D.W. Knight, C.K. Kiely and G.J. Hutchings, *Science*, 2011, **331**, 195; (b)W. Partenheimer, *Catal. Today*, 1995, **23**, 69; (c)R.L. Brutchey, I.J. Drake, A.T. Bell and T.D. Tilley, *Chem. Comm.*, 2005, **29**, 3736; (d)Y. Wang, H. Li, J. Yao, X. Wang and M. Antonietti, *Chem. Sci.*, 2011, **2**, 446.
- 3 (a)M. Ghaffarzadeh, M. Bolourtchian, M. Gholamhosseni and F. Mohsenzadeh, *Appl. Catal., A*, 2007, **333**, 131; (b)N. Tada, K. Hattori, T. Nobuta, T. Miura and A. Itoh, *Green Chem.*, 2011, **13**, 1669; (c)S.-I. Hirashima and A. Itoh, *Photochem. Photobiol. Sci.*, 2007, **6**, 521.
- 4 G. Pandey, R. Laha and D. Singh, *J. Org. Chem.* 2016, **81**, 7161.
- 5 A. Tanaka, K. Hashimoto and H. Kominami, *J. Am. Chem. Soc.*, 2012, **134**, 14526.
- 6 E. Fritz-Langhals and B. Kunath, *Tetrahedron Lett.*, 1998, **39**, 5955; A. Potthast, T. Rosenau, C.-L. Chen and J.S. Gratzl, *J. Org. Chem.*, 1995, **60**, 4320.
- 7 Y. Zhu, Y. Zhu, H. Zeng, Z. Chen, R.D. Little and C. Ma, *J. Electroanal. Chem.*, 2015, **751**, 105.
- 8 (a)Y. Wang, X. Wang and M. Antonietti, *Angew. Chem. Int. Ed.*, 2012, **51**, 68; (b)V. Augugliaro, M. Bellardita, V. Loddo, G. Palmisano, L. Plamiasano and S. Yurdakal, *J. Photochem. Photobiol., C*, 2012, **13**, 224.
- 9 (a)S. Yurdakal, G. Palmisano, V. Loddo, V. Augugliaro and L. Palmisano, *J. Am. Chem. Soc.*, 2008, **130**, 1568; (b)F. Su, S.C. Mathew, G. Lipner, X. Fu, M. Antonietti, S. Blechert and X. Wang, *J. Am. Chem. Soc.*, 2010, **132**, 16299.
- 10 P. Zhang, Y. Wang, H. Li, and M. Antonietti, *Green Chem.*, 2012, **14**, 1904.
- 11 (a)S. Verma, R.B.N. Baig, M.N. Nadagouda and R.S. Varma, *ACS Sustainable Chem. Eng.*, 2016, **4**, 2333; (b)Z. Ding, X. Chen, M. Antonietti and X. Wang, *ChemSusChem*, 2011, **4**, 274; (c)P. Zhang, Y. Gong, H. Li, Z. Chen, and Y. Wang, *RSC Adv.*, 2013, **3**, 5121.
- 12 W. Yi, R. Cao, W. Peng, H. Wen, Q. Yan, B. Zhou, L. Ma and H. Song, *Eur. J. Med. Chem.*, 2010, **45**, 639;
- 13 (a)A.W. Jackson, C. Stakes and D.A. Fulton, *Polym. Chem.*, 2011, **2**, 2500; (b) Y.-L. Zhao, Z. Li, S. Kabehie, Y.Y. Botros, J.F. Stoddart, and J.I. Zink, *J. Am. Chem. Soc.*, 2010, **132**, 13016; (c)D. Xiong, N. Yao, H. Gu, J. Wang, and L. Zhang, *Polymer*, 2017, **144**, 161.
- 14 (a)US Patent 5408009; (b) A. Burkhart, and H. Ritter, *Polym. Int.*, 2015, **64**, 329.
- 15 M. Ilkaeva, I. Krivtsov, E. Díaz, Z. Amghouz, Y. Patiño, S. Khainakov, J.R. García, S. Ordóñez, *J. Hazard. Mater.*, 2017, **332**, 59-69.
- 16 (a)P. Niu, L. Zhang, G. Liu and H.M. Cheng, *Adv. Funct. Mater.*, 2012, **22**, 4763. (b) I. Krivtsov, E. García-López, G. Marci, L. Plamiasano, Z. Amghouz, J.R. García, E. Díaz, S. Ordóñez, *Appl. Catal. B.*, 2017, **204**, 430-439.
- 17 T. Sano, S. Tsutsui, K. Koike, T. Hirakawa, Y. Teramoto, N. Negishi and K. Takeuchi, *J. Mater. Chem. A*, 2013, **1**, 6489.
- 18 Y. Zhang, A. Thomas, M. Antonietti and X. Wang, *J. Am. Chem. Soc.*, 2009, **131**, 50.
- 19 Y. Li, S. Ouyang, H. Xu, X. Wang, Y. Bi, Y. Zhang and J. Ye, *J. Am. Chem. Soc.*, 2016, **138**, 13289.
- 20 J. Li, B. Shen, Z. Hong, B. Lin, B. Gao and Y. Chen, *Chem. Commun.*, 2012, **48**, 12017.
- 21 B. Long, Z. Ding and X. Wang, *ChemSusChem.*, 2013, **6**, 2074.
- 22 S. Yurdakal and V. Augugliaro, *RSC Adv.*, 2012, **2**, 8375.
- 23 I. Yu. Chernyshov, M.V. Vener, P.V. Prikhodchenko, A. G. Medvedev, O. Lev, and A.V. Churakov, *Cryst. Growth Des.*, 2017, **17**, 214.
- 24 G. Chehardoliand M. A. Zolfigol, *Phosphorus, Sulfur Silicon Relat. Elem.*, 2010, **185**, 193.
- 25 M.X. Tan, L. Gu, N. Li, J.Y. Ying, Y. Zhang. *Green Chem.*, 2013, **15**, 1127.

## Tables

## Figure Captions

**Table 1** Substrates and the products of photo-oxidation reactions in the presence of TiO<sub>2</sub> and g-C<sub>3</sub>N<sub>4</sub> photocatalysts

substrate	oxidation products of P25 promoted reactions	oxidation products of TE and TE_O promoted reactions
	 Selectivity 8 %  Selectivity 10 %	 Selectivity 57 % (TE) Selectivity 82 % (TE_O)
		 Selectivity 39 % (TE) Selectivity 38 % (TE_O)
		
	 	 
	 	

**Table 2** MPET apparent reaction rate constant (k), conversion degree, HEB selectivity at 30% of MPET conversion

sample	k [min <sup>-1</sup> ]	MPET conversion after 4 h of the reaction [%]	HEB selectivity at 30 % of MPET conversion [%]
P25	0.0050	68	8
MCN	0.0029	50	50
TE	0.0060	75	57
TE_O	0.0052	72	82

**Table 3** SSA, BG and XPS data for MCN, TE, TE\_O data

sample	SSA [m <sup>2</sup> g <sup>-1</sup> ]	BG [eV]	XPS data		
			N2/N1 ratio	elemental composition	
				C/N	O [at%]
MCN	8	2.73	0.21	0.70	3.3
TE	154	2.80	0.20	0.71	3.7
TE_O	68	2.63/2.15	0.18	0.71	6.3

**Figure 1** Photooxidation of MPET in the presence of (●) MCN and (■) P25**Figure 2** MPET photooxidation in the presence of (●) TE and (◆) TE\_O. (A) MPET conversion, (B) HEB production, (C) HEB selectivity, (D) MPET conversion vs HEB selectivity**Figure 3** (A) PXRD patterns, (B) XPS O 1s, (C) 1H MAS NMR, and (D) FTIR, spectra of (blue) TE and (red) TE\_O samples**Figure 4** The model structures of: Left: «dimelem – MPET» complex. Right: «dimelem – H<sub>2</sub>O<sub>2</sub> – MPET» complex